Journal of Engineering and Technology for Industrial Applications

ITEGAM-JETIA

Manaus, v.12 n.57, p. 24-34. January/February, 2026.

DOI: https://doi.org/10.5935/jetia. v12i57.2679

ISSN ONLINE: 2447-0228

RESEARCH ARTICLE OPEN ACCESS

COMPARATIVE STUDY OF HMM AND BPNN IN DETECTING CORONA DISCHARGE ON 20 KV CUBICLE BASED ON VOLTAGE AND SOUND

Christiono Christiono*[1], Miftahul Fikri[2] and Syamsir Abduh[3]

[1, 2, 3]Institur Teknologi PLN. Jakarta, Indonesia.

[1]https://orcid.org/0000-0001-5457-9976, [2]https://orcid.org/0000-0002-9454-9197, [3]https://orcid.org/0009-0000-7984-8511

Email:*christiono@itpln.ac.id

ARTICLE INFO

Article History
Received: September 6, 2025
Revised: November 20, 2025
Accepted: January 1, 2026
Published: January 31, 2026

Keywords:
corona discharge,
20kV cubicle,
Voice
Hidden Markov Model (HMM),
Back Propagation Neural Network (BPNN),

ABSTRACT

Corona discharge is a common disturbance in 20 kV cubicles and may lead to insulation degradation, power losses, and potential equipment failure. Early detection is therefore essential to support preventive maintenance and enhance distribution system reliability. This study presents a comparative analysis of the Hidden Markov Model (HMM) and Backpropagation Neural Network (BPNN) for identifying corona discharge based on acoustic signals and voltage variations. Acoustic data were recorded using a needle–rod configuration and processed through Linear Predictive Coding (LPC) to obtain cepstral features. The classification results show that HMM provides high accuracy, achieving 100% in both training and testing for noise-based clustering and 84.44% in voltage-based testing. Meanwhile, BPNN demonstrates stable performance with training and testing accuracies of 95.93% and 82.35% for voltage-based clustering, and 95.69% and 100% for noise-based clustering, respectively. Overall, the findings indicate that although HMM performs more consistently for noise-based classification, BPNN provides competitive accuracy and better adaptability for early detection of corona discharge in 20 kV cubicles. These results support the development of intelligent monitoring systems for improving insulation condition assessment and reducing potential failures in medium-voltage distribution networks.

I. INTRODUCTION

Greater Jakarta is the center of electricity supply. PLN Distribution Jaya and UP3Cikokol have more nearly 7 million consumers, 11,564 MVA of installed power, and 12,426 distribution substations, according to PT PLN (Persero) figures from 2006. Cubicles and feeders are needed for three times as many distribution substations as there are substations.[1]**.** So, if done manually, the inspection in the context of maintenance will be very difficult. A voltage of 20 kV is applied to these cubicles, which can cause corona discharge symptoms and, if left unchecked, cause electrical failure or short circuits, especially under rain or humid environments[2]**.** If the repair is done immediately, the problem can be solved, but you can only find out the condition of the cubicle by visiting it[3]. Many people consider that corona discharge in a medium voltage cubicle (TM) is not enough to cause corona discharge.

However, the fact is that corona discharge can cause a flash jump, causing the cubicle to be unable to deliver electrical power [4]. Due to the high humidity level in Indonesia which allows air ionization to occur easily, the corona discharge problem in the TM cubicle is a unique and uncommon problem because the magnitude of the voltage (20 kV) is technically very difficult to cause corona discharge [5]. For example, PT. PLN (Persero) Jaya and Tangerang sustain more than 300 units of TM cube damage annually. Most of this damage is caused by the release of corona. Therefore, there needs to be a monitoring system that can see data from the entire room but can be accessed from the control center. With the latest condition data, technicians can immediately carry out maintenance to prevent more severe corona discharge, which can cause flashovers[6]. Figure 1 shows the structure and condition after cubicle damage.

(a) (b)

Figure 1: Cubicle Construction 20 kV Voltage (a) visible inside cubicle (b) visible part of the entire cubicle.
Source: Authors, (2026).

Figure 1 shows a 20 kV cubicle that suffered an insulation failure due to a previously unknown corona discharge phenomenon that caused permanent damage to its insulator. Part (a) shows the arrangement of the insulators inside the cubicle, and part (b) shows the overall cubic units; Both have suffered permanent damage due to insulation failure.

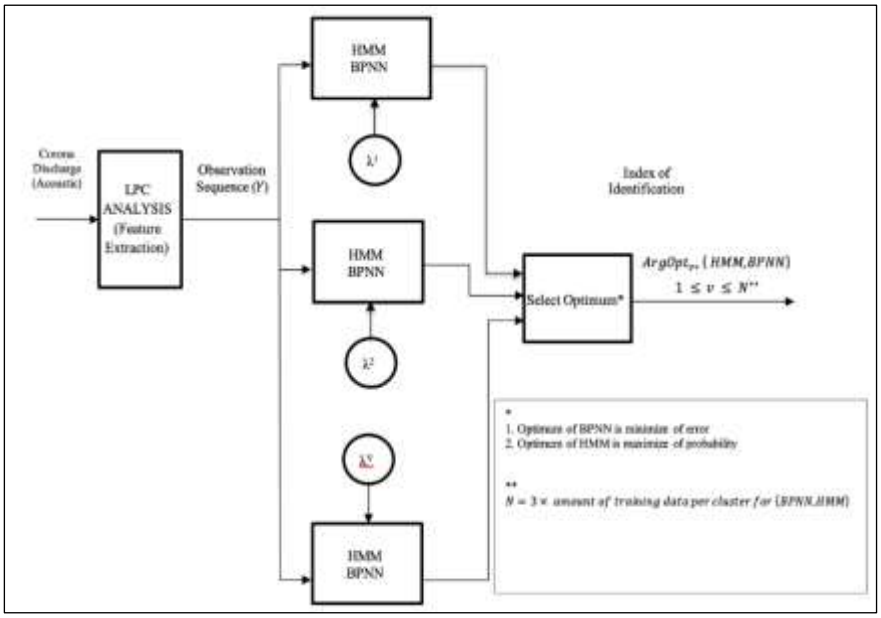

Figure 2: Acoustic Identification Flow Diagram of Corona Discharge Based on Voltage and Noise.
Source: Authors, (2026).

Any kind of medium-voltage or high-voltage electrode may cause corona discharge symptoms in specific situations.[7]. This is because an ionization process that can generate electrons or positive ions at 20 kV cubic insulation occurs when the electrode is subjected to an electric field. At some point, this collection of electrons or positive ions will form into an avalanche electron, which can then produce sound. The more the point group, the more interference the electrode produces. [8]. The noise level can be measured as a parameter of the magnitude of the level of corona discharge symptoms. This can be done by raising the voltage from 20 kV to 33 kV (less than the breakdown voltage).

Some corona discharge studies such as [9]. studying the loose corona on the transmission wire using loose partial measurement,[10]. Talking about corona discharge using unmanned aerial system technology,[11]. talking about how to classify corona discharge based on the pattern of partial discharge, [12]. detects corona discharge sound using fast Fourier transform. Then, using wavelet transformation to identify corona discharge signals based on the level of contamination or pollution. This signal is compared to a partial discharge detector measuring device. Recently, corona discharge sound clustering using geometric distance (ED) has been carried out.[13][14], using fuzzy c-mean (FcM) [15][16].and compare ED, FcM and hidden Markov model (HMM) methods [17].

However, AI uses backpropagation neural network (BPNN) to identify corona discharge sounds. In this study, clustering of the corona discharge phenomenon based on sound was carried out as a first step. This clustering is intended to identify early isolation failures in 20 kV cubicles using BPNN. The characteristic extraction of the recorded corona discharge sound is computed using the linear predictive coding (LPC) approach, which has long been recognized and proven to be dependable for obtaining characteristic extraction from any sound.After the extraction of these traits is obtained, matching is carried out using the BPNN and HMM methods to obtain clustering that is expected to be more accurate.

II. METHODOLOGY

In the acoustic observation of corona discharge, this study refers to IEEE Standard for High-Voltage Testing Techniques 4 2013-1995 IEEE [17] and IEC TS 62478:2016 High voltage test techniques - Measurement of partial discharges by electromagnetic and acoustic using PD data collection method. On the other hand, the use of needle-rod electrodes in vertical testing and microphone placement is at a distance of 3cm. With a standard frequency ranging between 40 and 200 kHz, this study used only 40 kHz. Each classification was done ten times in order to detect the acoustic phenomenon of corona ejection based on voltage and hissing sound. Preliminary observations show that the lowest penetration voltage is 34.3 kV, so the base voltage is clustered into 3 including: low cluster 20–24 kV, medium cluster 25–29 kV, and high cluster 30–33 kV, while sizzle noise is classified into pure Corona Discharger, Corona Discharger with hissing noise, and pure hissing noise. The humidity ranges from 70% to 95%, while the indoor temperature ranges from 27.5°C to 35.3°C. Data was gathered at the PLN Institute of Technology Jakarta's High Voltage Laboratory over a one-year observation period (February 2021–February 2022). The MATLAB Program version 2024b is then used to process the collected data. Figure 2 shows a flow diagram of the clustering of corona discharge phenomena based on acoustics.

II.1 PREDICTIVE LINEAR CODE

According to him, the LPC approach is a long-standing speech recognition methodology. [17]. The LPC method's benefits include its ease of use and compatibility with a wide range of devices. The two primary parts of the LPC method are encoding and decoding. While decoding modifies the recorded sound, encoding breaks down sound signals into their component elements. Here, both procedures are explained. Figure 3 [17].

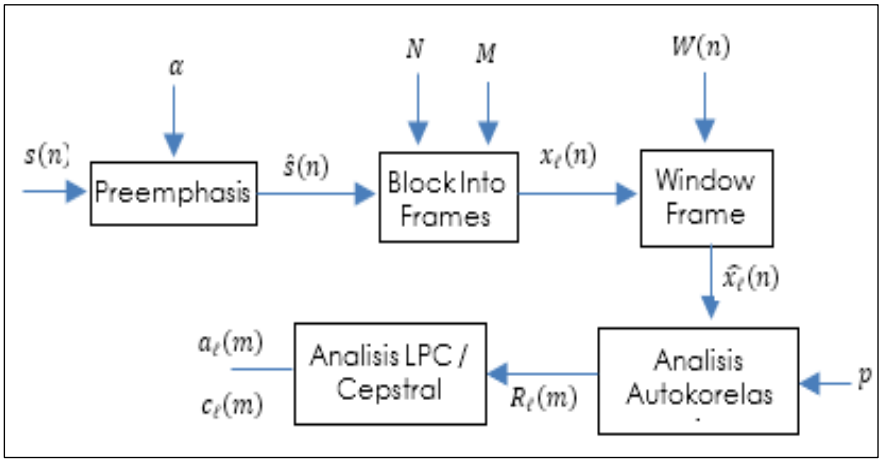

Figure 3: LPC Process as Acoustic Corona Release Feature Extraction.
Soucer: [13], [14], [16], [17].

with

$$\tilde{s}(n) = s(n) - \tilde{a}\, s(n-1), \tag{1}$$

where the acoustic data/signal,$sn$is the amount of data in an acoustic signal

$$0.9 \leq a \leq 1.$$
$$x_\ell(n) = \tilde{s}(M\ell + n) \tag{2}$$

where shows the number of frames,$M\ell = 1,2, \dots, M$.

$$\tilde{x}_\ell(n) = x_\ell(n)\, w(n), \tag{3}$$

Where$w(n) = 0.54 - 0.46 \cos\left(\frac{2\pi n}{N-1}\right), 0 \leq n \leq N-1$

$$r_\ell(m) = \sum_{n=0}^{N-1-m} \tilde{x}_\ell(n)\, \tilde{x}_\ell(n+m) \tag{4}$$

Where$m = 0,1, \dots, p$.

$$a_m = \alpha_m^{(p)} \tag{5}$$

with$1 \leq m \leq p$

$$E^{(0)} = r(0)$$

$$k_i = \frac{\left\{r(i) - \sum_{j=1}^{L-1} \alpha_j^{(i-1)} r(|i-j|)\right\}}{E^{(i-1)}}$$

$$\alpha_i^{(i)} = k_i$$

$$\alpha_j^{(i)} = \alpha_j^{(i-1)} - k_i \alpha_{i-j}^{(i-1)}$$

$$E^{(i)} = (1 - k_i^2)\, E^{(i-1)}$$

$$c_0 = \ln 1 \tag{6}$$

$$y_m = a_m + \sum_{k=1}^{m-1} \left(\frac{k}{m}\right) c_k a_{m-k} \tag{7}$$

Where$1 \le m \le p$.
The following explanation applies to the stages in Figure 2 above. [17]

- Acoustic noise from the original auditory input can be eliminated by the pre-emphasis method. Noise is interference or interference from the surrounding real hearing object.
- The frame-blocking process divides the acoustic signal into acoustic segments.
- Windowing detects and sorts out the differences in separate acoustic signals.
- Autocorrelation analysis ensures that the signals from each frame are comparable.
- The process of converting the magnitude of the LPC parameters—the logarithmic area ratio, reflection coefficient, and LPC coefficient—into the outcome of autocorrelation analysis is known as LPC analysis.
- Using a Fourier transform, the cepstral analysis converts the LPC parameter into a cepstral coefficient.

II.2 HIDDEN MARKOV MODEL

One of the secret Markov models is the Hidden Markov Standard Model (NHMM) $\{X_t, Y_t\}_{t\in\mathbb{N}}$Y which presupposes that it can be observed as long as its distribution is known to be normal. Unfollowed, the event's cause creates a Markov chain with the state space. The hidden Markov model's primary flaw is that it optimizes the Y observation process's potential function, which $Y_t X_t$ $\{X_t\}_{t\in\mathbb{N}}$ $S_X = \{1,2,\cdots,m\}$. [18][19] [17]

$$L_T(\phi) = P(Y_1 = y_1, Y_2 = y_2, \dots, Y_T = y_T|\phi)$$

$$= \sum_{i_1=1}^{m} \dots \sum_{i_T=1}^{m} \left(\pi_{y_1 i_1} \pi_{y_2 i_2} \dots \pi_{y_T i_T}\right) \times \left(\delta_{i_1} \gamma_{i_1 i_2} \gamma_{i_2 i_3} \dots \gamma_{i_{T-1} i_T}\right)$$

$$= \sum_{i_1=1}^{m} \dots \sum_{i_T=1}^{m} \delta_{i_1} \pi_{y_1 i_1} \prod_{t=2}^{T} \gamma_{i_{t-1} i_t} \pi_{y_t i_t}. \tag{8}$$

The acoustic properties of corona discharge, etc., were extracted in this work using the linear predictive coding (LPC) method. Parameter estimation, including mean, variance, and transition matrix, is performed to maximize the probability function. The Expectation Maximization (EM) algorithm is used iteratively to optimize the probability function in the equation (9). Each algorithm is formulated as follows.$y_1, y_2, \dots, y_T$[19]. [17]

$$\mu_i^{(k+1)} = \frac{\sum_{t=1}^{T} \alpha_t^{(k)}(i) \beta_t^{(k)}(i) y_t}{\sum_{t=1}^{T} \alpha_t^{(k)}(i) \beta_t^{(k)}(i)}, \tag{9}$$

$$\sigma_i^{2(k+1)} = \frac{\sum_{t=1}^{T} \alpha_t^{(k)}(i) \beta_t^{(k)}(i) \left(y_t - \mu_i^{(k+1)}\right)^2}{\sum_{t=1}^{T} \alpha_t^{(k)}(i) \beta_t^{(k)}(i)} \tag{10}$$

$$\gamma_{ij}^{(k+1)} = \frac{\sum_{t=1}^{T-1} \alpha_t^{(k)}(i) \gamma_{ij}^{(k)} P^{(k)}(y_{t+1}|j) \beta_t^{(k)}(j)}{\sum_{t=1}^{T-1} \alpha_t^{(k)}(i) \beta_t^{(k)}(i)} \tag{11}$$

Forward and backward algorithms can be used to calculate recursivelyand Furthermore, these findings are used to divide the corona release phenomenon based on voltage and interference taking into account the maximum probability.$\alpha_t(i) = P(Y_1 = y_1, Y_2 = y_2, \dots, Y_t = y_t, X_t = i|\phi)$ $\beta_t(i|\phi) = P(Y_{t+1} = y_{t+1}, \dots, Y_T = y_T|X_t = i, \phi)$.

II.3 BACKPROPAGATION NEURAL NETWORK (BPNN)

The backpropagation neural network (BPNN), an artificial intelligence technique that uses optimization to reduce the function of the objective—that is, the difference between the experimental and model data—is applied to model data based on experimental data. Figure 4 below shows the BPNN architecture. [20][21]:

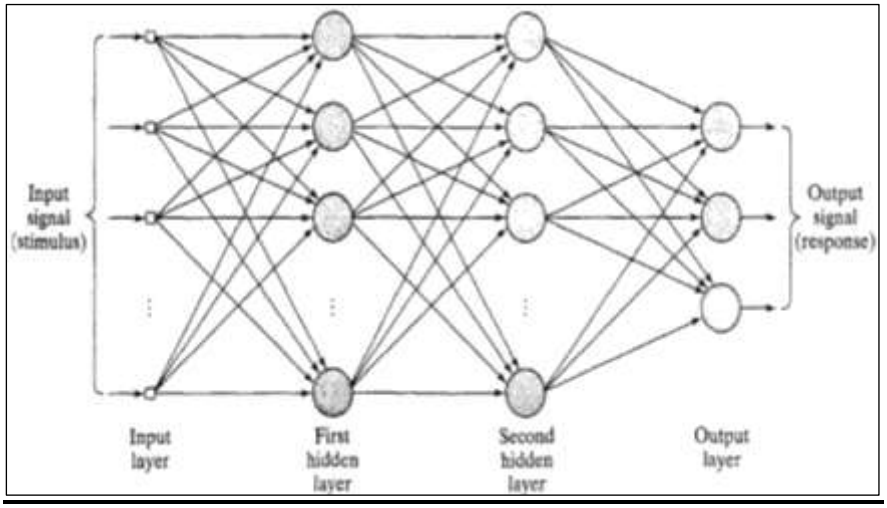

Figure 4: BPNN Architecture.
Source: Authors, (2026).

The objective functions of BPNN are as follows:

$$\xi = \frac{1}{2}\sum_{j\in C} e_j^2(n) \tag{12}$$

with , with is the output signal of BPNN is the experimental output data of the same input. $e_j(n) = d_j(n) - y_j(n) y_j(n)\, d_j(n).$

BPNN learning is achieved by entering the observation data into the BPNN and then reducing errors along with estimating BPNN parameters that match the weight, as shown in Figure 4. To minimize errors in equations (12), various optimization methods are used.

Table 1: Connected functions of the BPNN model.

Connected function	Schema
	BPNN
$z_{in} = f_1 = f_1(X^*, b1, v)$	$b1 + X\ v$
$z = f_2 = f_2(z_{in})$	$\frac{1}{(1 + exp(-z_{in}))}$
$y_{in} = f_3 = f_3(z, b2, w)$	$b2 + z\ w$
$(\alpha, \beta) = f_4 = f_4(y_{in})$	-
$T^* = L = L(\alpha, \beta, C, E, n)$	-
$T^* = f_5 = f_5(y_{in})$	y_{in}
n_1	4
n_2	1

Source: Authors, (2026).

with lifetime input and data$X^*T^{\#}$ [22], the research model for and BPNN in this case is as follows:

$$T^* = f_5\ o\ f_3\ o\ f_2\ o\ f_1 \qquad for\ BPNN \tag{13}$$

In this model, the parameters is b1,v,b2,w for the BPNN scheme.

II.4 PARAMETER MODEL ESTIMATION

To gain a better grasp of the formulation of the model parameters in Table 1, the GD approach is then used to optimize the function based on its objective in equation (13). is the function of the objective model in equation (6), and the model construction is shown in Table 2.T^* Genetic algorithms have phases and function similarly to genes. [23] [24] Initialization, spin wheel, cross-over, mutation, individual assessment, and linear fitness improvement. All of these procedures are executed by default, with the exception of the individual evaluation phase. Change the objective function now in accordance with Table 1 based on [23] [25].

The evolutionary algorithm's stages (1) through (6) guarantee that the BPNN approaches converge, meaning that the model's results get smaller with each iteration, reducing the gap between the experiment and the model. Based on [26][27], to guarantee convergence and minimize errors between models and experimental data. The convergence of the LM technique for BPNN will thus be guaranteed by the modified parameters. Put another way, as the number of iterations increases, the gap between the experiment's and the model's outcomes will narrow. The following table 2 illustrates the entire procedure:

Table 2: Parameters of BPNN Formulation.

Formulation BPNN
$w_{ji}(n+1) = w_{ji}(n) - \alpha e_j(n+1)\, z, \qquad b2_i(n+1) = b2_i(n) - \alpha e_j(n+1),$
$v_j(n+1) = v_j(n) - \alpha e_j(n+1)\left(\frac{1}{(1+exp(-z_{in}))}\frac{exp(-z_{in})}{(1+exp(-z_{in}))}\right) X,$
$b1_j(n+1) = b1_j(n) - \alpha e_j(n+1)\left(\frac{1}{(1+exp(-z_{in}))}\frac{exp(-z_{in})}{(1+exp(-z_{in}))}\right),$
is scalar (learning rate).α

Soucer: [24], [28-31].

III. RESULTS AND DISCUSSION

III.1 DESIGN AND OBSERVATION SERIES

The design and series of observations made can be seen in figures 5 and 6 below.

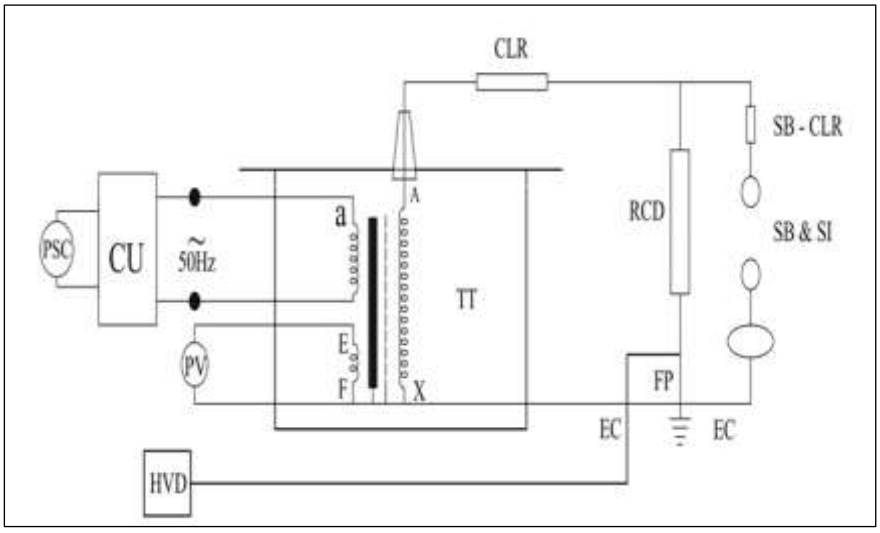

Figure 5: Corona Discharge Acoustic Recording Series in 20 kV Cubic.
Source: Authors, (2026).

Figure 6: Research Design for Acoustic Recording of Corona Discharge in a 20 kV Cubicle.
Source: Authors, (2026).

Figure 6 displays the acoustic recording of corona discharge in the High Voltage Oratory Lab at the PLN Institute of Technology. It is generated by a test transformer that can be adjusted to 100 kV and has a 200 V scale ratio. According to the findings of the preliminary observations, the corona discharge's penetration voltage was 34.3 kV. In order to create three clusters, the acoustic recording of corona discharge in this investigation started at a voltage of 20 kV and was thereafter increased gradually. Furthermore, three types of CDs were used to capture the acoustic data: pure CDs, CDs with noise, and CDs with pure noise. The temperature in the room increased from 27.5 to 35.3 degrees Celsius over the data collecting period, and the humidity ranged from 70% to 95%. The corona discharge is recorded acoustically between the two electrodes, which are spaced three centimeters apart.[11]. The microphone is positioned 5 cm away from the electrodes for acoustic recording, and the recordings are saved on a computer for analysis.[32]

III.2 ACOUSTIC CORONA EMISSION DATA AND EXTRACTION

With each pure CD cluster, corona acoustic dissipation was recorded using the research design depicted in figure 5 according to sound and voltage (20–24 kV, 25–29 kV, and 30-33 kV). Figure 6 displays CDs with sound and CDs with only sound. [17]

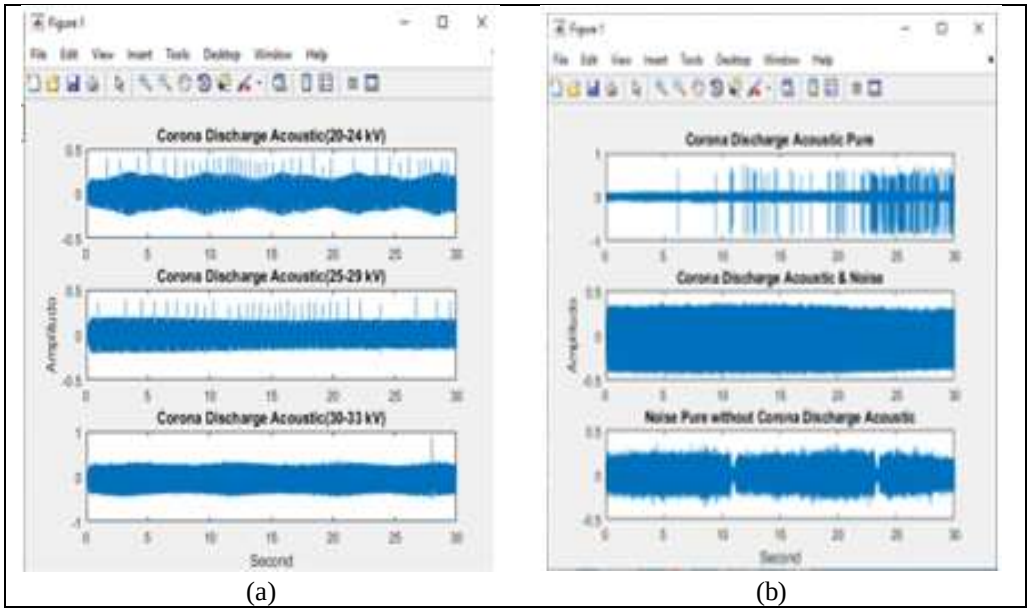

(a) (b)

Figure 7: Acoustic Coronas Discharge (a) Based on Voltage (b) Based on Noise.
Source: Authors, (2026).

Using equations (1)–(5), the acoustic data in Figures 7 (a) and 6 (b) were calculated to yield the LPC parameters. Moreover, Fourier transformations do a better job of extracting the acquired features.[16]. utilizing equations (6)–(7), which yields Figure 7(a) and 7(b)'s cepstral coefficient of LPC.

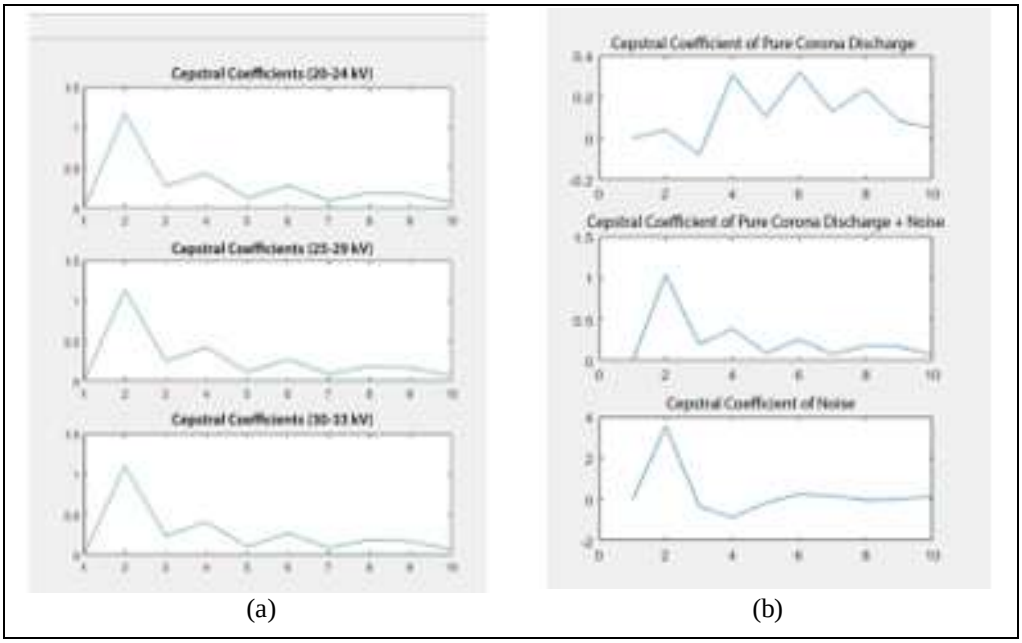

(a) (b)

Figure 8: Cepstral Coefficient LPC Acoustic Corona Discharge (a) Based on Voltage (b) Based on Noise.
Source: Authors, (2026).

Figure 8(a) is comparable in that there are no outside disturbances, or noises, so it can only produce sufficient results[17]. In contrast, Figure 8(b) is very different because of the sound effect, so it is expected to produce precise grouping results. Furthermore, the extraction of the cepstral LPC feature was used as an input for the Euclidean, HMM, and BPNN distance methods to identify and classify the corona acoustic discharge.

Table 3: Acoustic Identification Accuracy of CDs by Voltage Using HMM.

NOT.	Training		Testing	
	Amount of Data	Accuracy (%)	Amount of Data	Accuracy (%)
1	1	100	9	88.89
2	2	100	8	83 . 33
3	3	100	7	80 . 95
4	4	100	6	77 . 78
5	5	100	5	73. 33
6	6	100	4	91. 67
7	7	100	3	88,89
8	8	100	2	100
9	9	100	1	100
Average	**100%**		**84,44%**	

Source: Authors, (2026).

Table 3 demonstrates how to use an HMM to identify acoustic CDs based on voltage. They achieved 100% accuracy throughout training and 84.44% accuracy during testing.

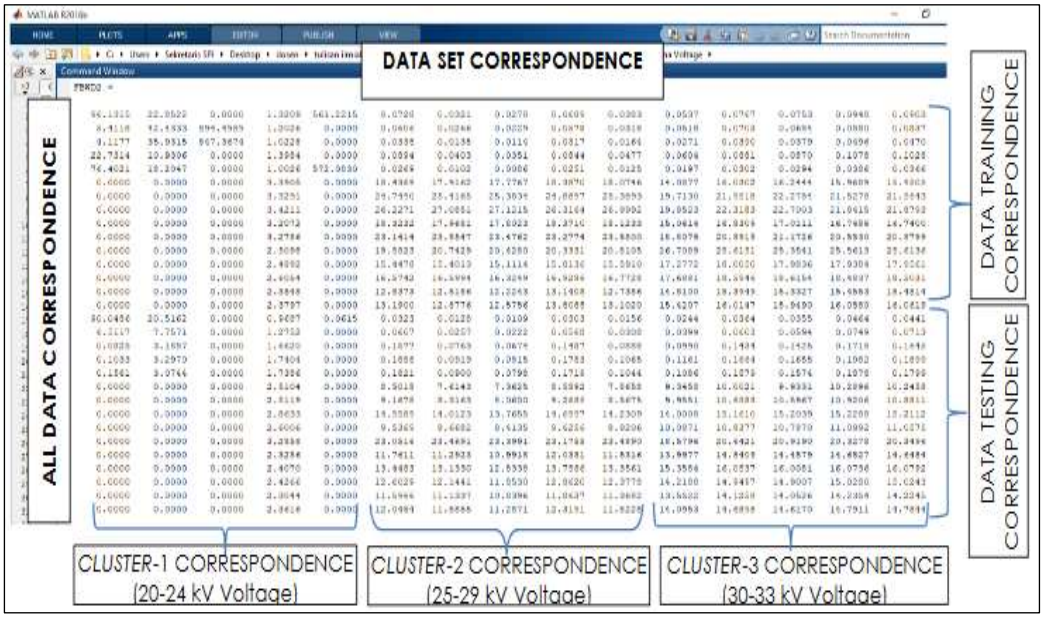

Figure 9: dentification of CD Acoustic Based on Voltage using hidden Markov models.
Source: Authors, (2026).

Table 4: Acoustic Identification Accuracy of CDs Based on Noise Using HMM.

NOT.	Training		Testing	
	Amount of Data	Accuracy (%)	Amount of Data	Accuracy (%)
1	1	100	9	100
2	2	100	8	100
3	3	100	7	100
4	4	100	6	100
5	5	100	5	100
6	6	100	4	100
7	7	100	3	100
8	8	100	2	100
9	9	100	1	100
Average	**100%**		**100%**	

Source: Authors, (2026).

Table 4 demonstrates how to use an HMM to identify CDs acoustically based on noise. They achieved 100% accuracy for both testing and training.

Table 5: Acoustic Identification Accuracy of CDs by Voltage Using BPNN.

NOT.	Training		Testing	
	Amount of Data	Accuracy (%)	Amount of Data	Accuracy (%)
1	1	99.99	9	95.00
2	2	90.00	8	65.55
3	3	98.50	7	90.20
4	4	91.10	6	70.00
5	5	99.05	5	82.35
6	6	93.33	4	98.00
7	7	97.77	3	75.10
8	8	95.63	2	88.95
9	9	98.00	1	76.00
Average	95.93%		82.35%	

Source: Authors, (2026).

Table 5 demonstrates how to use an BPNN to identify acoustic CDs based on voltage. They achieved 95.93% accuracy throughout training and 82.35% accuracy during testing.

Table 6: Acoustic Identification Accuracy of CDs by Noise Using BPNN.

NOT.	Training		Testing	
	Amount of Data	Accuracy (%)	Amount of Data	Accuracy (%)
1	1	98.90	9	100
2	2	90.50	8	100
3	3	99.50	7	100
4	4	91.11	6	100
5	5	99.99	5	100
6	6	92.20	4	100
7	7	98.80	3	100
8	8	93.00	2	100
9	9	97.21	1	100
Average	95.69%		100%	

Source: Authors, (2026).

Table 6 demonstrates how to use an BPNN to identify CDs acoustically based on noise. They achieved 95.69% accuracy for both testing and and 100% accuracy during testing.

Table 7: Recapitulation of CD Acoustic Base Voltage and Noise Using HMM and BPNN.

NOT.	**Method**	**Accuracy Mean (%)**			
		Base Voltage		**Base Noise**	
		Training	Testing	Training	Testing
1	HMM	100	84.44	100	100
2	BPNN	95.93	82.35	95.69	100

Source: Authors, (2026).

Table 7 presents a comparison of the accuracy of the HMM and BPNN methods in classifying Base Voltage and Base Noise conditions in CD acoustic data. HMM shows very high accuracy, particularly for Base Noise, achieving 100% accuracy in both training and testing, while its testing accuracy for Base Voltage reaches 84.44%. BPNN also demonstrates good performance, with training and testing accuracies of 95.93% and 82.35% respectively for Base Voltage, and stable results for Base Noise with 95.69% during training and 100% during testing. Overall, HMM appears more consistent, especially for the Base Noise parameter, although BPNN remains competitive for both parameters.

IV. CONCLUSIONS

This study evaluates the performance of the Hidden Markov Model (HMM) and Backpropagation Neural Network (BPNN) in detecting corona discharge phenomena in 20 kV cubicles using acoustic signals and voltage-based clustering. The application of Linear Predictive Coding (LPC) successfully extracts cepstral features from the recorded corona discharge sounds, enabling effective classification. The results show that HMM achieves outstanding performance for noise-based clustering, reaching 100% accuracy in both training and testing, while its voltage-based testing accuracy reaches 84.44%. In contrast, BPNN provides more balanced and stable results across all categories, with accuracies of 95.93% (training) and 82.35% (testing) for voltage-based clustering, and 95.69% (training) and 100% (testing) for noise-based clustering. These findings highlight that although HMM excels in noise classification, BPNN offers robust performance and better generalization capability for both voltage and noise conditions. Therefore, BPNN is recommended as a reliable early warning method for corona discharge detection in 20 kV cubicles, contributing to improved monitoring, preventive maintenance, and overall distribution network reliability.

V. AUTHOR'S CONTRIBUTION

The authors assisted in the development of a system that detects corona discharge symptoms in 20 kV cubicles using artificial intelligence methods. The authors of this study compared Hidden Markov Model (HMM) and Backpropagation Neural Network (BPNN) techniques to identify sounds resulting from corona discharge symptoms. The authors not only conducted experiments in a high-voltage laboratory to collect sound data, but they also processed the data using the Linear Predictive Coding (LPC) method to identify sound characteristics. The results showed that BPNN can improve identification accuracy compared to HMM. Consequently, BPNN can be used as a more accurate early warning system. This is very important because PLN and related agencies can help detect damage to cubicles quickly, prevent further damage to equipment and improve the reliability of electricity distribution.

VI. ACKNOWLEDGMENTS

The authors would like to thank the PLN Institute of Technology, Jakarta, especially the High Voltage Laboratory, for providing the facilities and opportunity to conduct this research. Appreciation is also extended to fellow lecturers and researchers who assisted in the data collection process and provided valuable input throughout the research.

VII. AUTHOR'S CONTRIBUTION

Conceptualization: Christiono Christiono, Miftahul Fikri and Syamsir Abduh.
Methodology: Christiono Christiono, Miftahul Fikri and Syamsir Abduh.
Investigation: Christiono Christiono, Miftahul Fikri and Syamsir Abduh.
Discussion of results: Christiono Christiono, Miftahul Fikri and Syamsir Abduh.
Writing – Original Draft: Christiono Christiono, Miftahul Fikri and Syamsir Abduh.
Writing – Review and Editing: Christiono Christiono, Miftahul Fikri and Syamsir Abduh.
Resources: Christiono Christiono, Miftahul Fikri and Syamsir Abduh.
Supervision: Christiono Christiono, Miftahul Fikri and Syamsir Abduh.
Approval of the final text: Christiono Christiono, Miftahul Fikri and Syamsir Abduh.

VIII. REFERENCES

[1] I. E. Portuguese et al., "RF-based partial discharge early warning system for air-insulated substations," IEEE Trans. Power Deliv., vol. 24, no. 1, pp. 20–29, 2009, doi: 10.1109/TPWRD.2008.2005464.

[2] X. Wang, N. Taylor, and H. Edin, "Effect of humidity on partial discharge in a metal-dielectric air gap on machine insulation and trapezoidal testing voltages," J. Electrostat., vol. 83, pp. 88–96, 2016, doi: 10.1016/j.elstat.2016.08.003.

[3] R. Syahbana, "Analysis of the Formation of Corona in a 20Kv Voltage Cubicle Channel and Its Effect on Power Losses," Lens, vol. 2, no. 48, pp. 14–21, 2019.

[4] R. Masarrang, Lily Stiowaty Patras, and Hans Tumaliang, "Rudolfus Masarrang," J. Tek. Electrical and Computer., vol. 8, no. 2, pp. 67–74, 2019.

[5] and S. K. A. S. Menesy, X. Jiang, M. A. Ali, H. M. Sultan, N. M. Alfakih, "Partial Discharge and Breakdown Characteristics in Small Air Gap Length Under DC Voltage in Needle-Plane Electrode Configuration," pp. 869–874, 2020.

[6] X. Li, J. Wang, T. Lu, and X. Cui, "Statistical analysis of audible noise generated by AC corona discharge from single corona sources," High Volt., vol. 3, no. 3, pp. 207–216, 2018, doi: 10.1049/hve.2017.0159.

[7] A. Syakur and U. Diponegoro, "Measurement of Air Dielectric Penetration Voltage in Various Cells," J. Thesis, no. January 2011, 2016.

[8] C. Widyastuti, I. N. Bagus, and Y. Dharma, "Energy and Electricity: A Scientific Journal of the Impact of Corona on 500 kV SUTET on Radio Interference of Energy and Electricity: A Scientific Journal," J. Ilm., vol. 11, no. 2, pp.
87–97, 2019.

[9] S. Hedtke, M. Pfeiffer, and C. M. Franck, "Corona discharge pulse pattern and audible noise on hybrid AC/DC transmission lines under electric field bias, ripple and ion coupling," J. Electrostat., vol. 102, 2019, doi:
10.1016/j.elstat.2019.103373.

[10] A. J. Moore, M. Schubert, and N. Rymer, "Technologies and Operations for High Voltage Corona Detection with UAVs," IEEE Power Energy Soc. Gen. Meet., vol. 2018-Aug, 2018, doi: 10.1109/PESGM.2018.8585759.

[11] M. Karimi, M. Majidi, H. Mirsaeedi, M. M. Arefi, and M. Oskuoee, "A novel application of deep belief networks in learning partial discharge patterns for classifying corona, surface, and internal discharges," IEEE Trans. Ind. Electron., vol. 67, no. 4, pp. 3277–3287, 2020, doi: 10.1109/TIE.2019.2908580.

[12] M. Wahyudi, Tumiran, I. M. Yulistya Negara, N. Akhmad Setiawan, and B. Sugiyantoro, "Audiosonic Acoustic Detection of Air Corona Discharge based on Fast Fourier Transform," Proc. 2nd Int. Conf. High Volt. Eng. Power Syst. Towar. Sustain. Reliab. Power Deliv. ICHVEPS 2019Pp. 1–6, 2019, doi: 10.1109/ICHVEPS47643.2019.9011029.

[13] M. FIKRI, C. CHRISTIONO, and I. G. MULYANA K., "Clustering of Corona Discharge Phenomena based on Sound using LPC and Euclidean Distance Methods," ELKOMIKA J. Tek. Electric Energy. Tech. Telecommunications. Tech. Electron., vol. 10, no. 3, p. 689, 2022, doi: 10.26760/elkomika.v10i3.689.

[14] N. PASRA, M. FIKRI, K. T. MAURIRAYA, T. RIJANTO, and I. G. P. A. BUDITJAHJANTO, "Noise Detection of Corona Discharge Sound based on Noise using LPC and Euclidean Distance Methods," ELKOMIKA J. Tek. Electric Energy. Tech. Telecommunications. Tech. Electron., vol. 11, no. 1, p. 72, 2023, doi: 10.26760/elkomika.v11i1.72.

[15] Mr. Fikri et al., "Optimization Objective Function Corona Discharge Acoustic Using Fuzzy C-Means (FcM)," Elkha, vol. 15, no. 2, p. 84, 2023, doi: 10.26418/elkha.v15i2.63601.

[16] Mr. FIKRI et al., "Clustering of Corona Discharge Sounds by Voltage using the Fuzzy C-Mean Method," ELKOMIKA J. Tek. Electric Energy. Tech. Telecommunications. Tech. Electron., vol. 11, no. 3, p. 609, 2023, doi: 10.26760/elkomika.v11i3.609.

[17] Mr. Fikri et al., "COMPARISON OF CORONA DISCHARGE IDENTIFICATION IN 20 kV CUBICLES BASED ON VOLTAGE AND NOISE USING ED, HMM, AND FCM," J. Techno., vol. 86, no. 5, pp. 11–22, 2024, doi: 10.11113/jurnalteknologi.v86.19986.

[18] M. FIKRI, B. SETIAWATY, and I. G. P. PURNABA, "Parameter Estimation and Congenescence of Parameter Estimation of the Poisson Hidden Markov Model," J. Math. Its Appl., vol. 15, no. 1, pp. 45–54, 2016, doi: 10.29244/jmap.15.1.45-54.

[19] M. Fikri, Samsurizal, Christiono, and K. T. M, "Weather Modeling Using the Hidden Markov Model for Solar Energy Utilization," Lightning, vol. 9, no. 2, pp. 217–224, 2020.

[20] M. D. Engelhart and H. Moughamian, "Book Reviews: Book Reviews," Educ. Psychol. Stuff., vol. 28, no. 3, pp. 951–951, 1968, doi: 10.1177/001316446802800332.

[21] S. Haykin, Neural Networks - A Comprehensive Foundation, Second. Pearson Prentice Hall, 1988.

[22] Z. Ma, L. Yang, H. Bian, M. S. Bhutta, and P. Xu, "An Improved IPM for Life Estimation of XLPE under DC Stress Accounting for Space-Charge Effects," IEEE Access, vol. 7, pp. 157892–157901, 2019, doi: 10.1109/ACCESS.2019.2946521.

[23] Mr. Melanie, An Introduction to Genetic Algorithms. Cambridge: MIT Press, 1996.

[24] Mr. Fikri et al., "Lifetime estimation of DC XLPE cable insulation using BPNN-IPM improved with various schemes and optimization methods," Indonesian. J. Electr. Eng. Comput. Sci., vol. 36, no. 1, pp. 86–98, 2024, doi: 10.11591/ijeecs.v36.i1.pp86-98.

[25] S. Mirjalili, Evolutionary Algorithms and Neural Networks. Cham: Springer Nature, 2019.

[26] H. B. Nielsen, "Imm Department of Mathematical Modelling Damping Parameter in Marquardt'S Method," no. M, 1999.

[27] C. Kanzow, N. Yamashita, and M. Fukushima, "Levenberg-Marquardt methods with strong local convergence properties for solving nonlinear equations with convex constraints," J. Comput. Appl. Math., vol. 173, no. 2, pp. 321–343, 2005,
doi: 10.1016/j.cam.2004.03.015.

[28] R. P. Lippmann, "An introduction to computing with neural nets," ACM SIGARCH Comput. Archit. News, vol. 16, no. 1, pp. 7–25, 1988, doi: 10.1145/44571.44572.

[29] S. Kusumadewi and S. Hartati, NEURO-FUZZY Integration of Fuzzy Systems and Neural Networks. Yogyakarta: Graha Ilmu, 2006.

[30] R. P. Lippmann, "An Introduction to Computing with Neural Nets," IEEE ASSP Mag.Pp. 4–22, 1987.

[31] D. E. Rumelhart and G. E. Hintont, "Learning representations by back-propagating errors," Nature, vol. 323, no. 9, pp. 533–536, 1986.

[32] Y. Liu, J. Xv, Y. Liu, H. Yuan, and Y. Cui, "A Method for the Indirect Detection of Audible Noise from High-Voltage Direct Current Transmission Lines," IEEE Trans. Instrument. Stuff., vol. 69, no. 7, pp. 4358–4369, 2020, doi: 10.1109/TIM.2019.2942251.